Letter

Safety-Critical Trajectory Tracking for Mobile Robots With Guaranteed Performance

Wentao Wu, *Graduate Student Member, IEEE*, Di Wu, *Member, IEEE*, Yibo Zhang, *Member, IEEE*, Shukang Chen, and Weidong Zhang, *Senior Member, IEEE*

Dear Editor,

This letter considers a collision-free trajectory tracking problem for performance-guaranteed mobile robots (MRs) subject to obstacles. We propose a safety-critical performance-guaranteed trajectory tracking method based on control barrier functions (CBFs). First, an auxiliary system is established to generate the non-negative signals for inflexible bounds such that the performance constraints are not violated when avoiding obstacles. Next, the desired guidance laws are devised to evolve tracking errors within performance space by the error transformation technique. Then, a position-heading CBF based on a heading collision-free principle is developed. Under the CBF framework, the safety-critical angle speed guidance law is solved by a quadratic program with respect to position-heading CBF constraints. It is proved that all errors can converge and evolve within a prescribed performance space, and the closed-loop system is ensured to be safe. Finally, simulation and experiment results are given to verify the effectiveness and feasibility of the proposed control scheme.

Relative works: The mobile robot (MR) has become an increasingly concerning topic due to its intelligence, automation, and collaboration with various applications, such as exploration, surveillance, transportation, and search and rescue [1]–[5]. As MR becomes more prominent, it is important to ensure that MR not only performs efficiently but also operates safely in complex environments.

In terms of performance indices, [6] proposed a prescribed performance control (PPC) scheme for a linearizable nonlinear system to specify the transient and steady-state indices explicitly. With the increasing popularity in multi-agent systems, the PPC methodology has been applied not only to enhance the performance of controlled systems [7]–[10], but also to guarantee the safety of formations [11], [12]. In particular, [7] studied the disturbance attenuation PPC tracking problem of wheeled MRs subject to skidding, slipping and input disturbance, which are estimated by a sliding-mode disturbance observer. For unknown and bounded uncertainties with unknown bounds, [8] developed an adaptive robust PPC scheme with the emulated uncertainty bounds. For the unavailable velocities, [9] proposed a fuzzy state observer-based finite-time control method for a performance-guaranteed time-varying formation under an undirected graph. Using universal barrier Lyapunov functions, [10] designed a singularity-free fixed-time prescribed performance method for nonholonomic MRs to implement a rigidity graph-based maneuvering. In [7]–[10], it is not considered that the potential collision risk is caused by neighboring robots, which will pose a critical and challenging mission for the MR's safety. In [11], a leader-follower PPC safe formation control method is derived for full-actuated surface vehicles by establishing a safety error transformation function (ETF). In [12], a fixed-time vision-based formation control protocol for MRs is proposed under field-of-view and performance constraints. References [11], [12] can achieve performance-guaranteed tracking control without collisions among neighboring robots. It is observed that prescribed performance functions in [7]–[12] are inflexible. The inflexible boundaries cannot accommodate error fluctuations due to obstacle avoidance and deal with the safety problem of MRs subject to environmental obstacles.

More recently, control barrier functions (CBFs) are increasingly applied to address the safety-critical control problem, such as adaptive cruise control [13], lane keeping [13], and collision-free formations [14]–[18]. The CBF-based safety-critical framework aims to synthesize controllers for ensuring the safety of nonlinear systems. According to [14]–[18], the safety-critical controller constraints may force the system states or tracking errors to deviate from the origin. However, fluctuant states or errors may violate the PPC constraints because the safety objective takes priority over the stability performance.

Motivated by above discussions, this letter aims to develop a safety-critical trajectory tracking method with guaranteed performance for MRs subject to dynamics and stationary obstacles. The main highlights of this letter are stated below: 1) Compared with existing PPC results [7]–[12], a flexible performance function (FPF) is developed by establishing an auxiliary system based on the relative distance between MR and obstacles. The designed FPF can tolerate the fluctuant errors by automatically enlarging or recovering boundaries, which is impossible for standard PPC techniques [7]–[12]. 2) Different from relative position-based CBFs in [15]–[18], we design a position-heading CBF based on the heading collision-free principle, which can implement the avoidance action by only adjusting the angle speed. Under the CBF framework, the FPF-based desired angle speed is modified to devise a safety-critical angle speed with a minimal cost under position-heading CBF constraints. Compared with the collision-free PPC schemes in [11], [12], our proposed method can handle both stationary and dynamic obstacles without violating FPF constraints.

Problem statement: Let x, y, φ, u, and w denote the positions, heading, surge, and angular speeds of MRs, respectively. Then, the kinematics of MRs is expressed as [19]

$$\dot{p} = R(\varphi)u,\ \ \dot{\varphi} = w,\ \ R(\varphi) = [\cos\varphi, \sin\varphi]^T \tag{1}$$

with $p = \mathrm{col}(x, y)$, where $\mathrm{col}(\cdot)$ denotes a column vector.

To implement the trajectory tracking, relative distance and heading errors e_1 and e_2 are defined as follows:

$$e_1 = \sqrt{x_e^2 + y_e^2},\ \ e_2 = \varphi_d - \varphi \tag{2}$$

where $x_e = x_d - x$ and $y_e = y_d - y$ with $p_d = \mathrm{col}(x_d, y_d)$ being a predefined reference trajectory; $\varphi_d = \mathrm{atan2}(y_e, x_e)$ denotes a desired heading angle, where $\mathrm{atan2}(\cdot,\cdot) \in (-\pi, \pi]$ is a four quadrant inverse tangent function [20], [21].

It is assumed that MR moving along p_d may encounter obstacles, which can be modeled as a closed circular area with a center $p_o = \mathrm{col}(x_o, y_o)$ and the radius $R_o \in \mathbb{R}^+$. This paper aims to develop a safety-critical trajectory tracking method for MRs with guaranteed performances such that: 1) The errors e_1, e_2 can converge and evolve within a constraint space while avoiding collisions. 2) It ensures the safety of MR, i.e., $\|p - p_o\| \geq R_o + \rho_o$ with ρ_o being a positive scaling parameter.

Design and analysis: This part designs the safety-critical trajectory tracking method for MRs under guaranteed performance. The stability and safety of closed-loop system are analyzed.

Flexible performance functions: To improve the tracking performance of underactuated MRs, we formulate the tracking errors e_i, $i = 1, 2$ such that

$$-e_{il} < e_i < e_{ir},\ \ i = 1, 2 \tag{3}$$

where $e_{ir} = (\delta_{ir} + \mathrm{sign}(e_i(t_0)))\varrho_i(t) - \varrho_{i\infty}\mathrm{sign}(e_i(t_0))$ and $e_{il} = (\delta_{il} - \mathrm{sign}(e_i(t_0)))\varrho_i(t) + \varrho_{i\infty}\mathrm{sign}(e_i(t_0))$ with $0 \leq \delta_{ir}, \delta_{il} \leq 1$; $\varrho_i(t) = (\varrho_{i0} - \varrho_{i\infty})e^{-\mu_i(t-t_0)} + \varrho_{i\infty}$ with $\varrho_{i0} = \varrho_i(t_0) > \varrho_{i\infty} = \lim_{t\to\infty}\varrho_i(t)$, and $\mu_i \in \mathbb{R}^+$. Note that ψ_d is not well defined when $e_1 = 0$ due to no definition of $\mathrm{atan2}(0, 0)$. According to non-negativeness of e_1, ψ_d can be well defined if $e_1 > 0$ for $\forall t > t_0$. Thus, one has $e_{1l} = 0$ with $\delta_{1l} = 1$ and $\varrho_{1\infty} = 0$.

Noticing that constraint (3) has inflexible bounds, error e_i may violate the constraint (3) due to collision avoidance. Thus, modified signals $\eta_{ir} \geq 0$ and $\eta_{il} \geq 0$ are introduced into (3) to obtain the adjustable bounds called FPF

Corresponding authors: Yibo Zhang and Weidong Zhang.

Citation: W. Wu, D. Wu, Y. Zhang, S. Chen, and W. Zhang, "Safety-critical trajectory tracking for mobile robots with guaranteed performance," *IEEE/CAA J. Autom. Sinica*, vol. 11, no. 9, pp. 2033–2035, Sept. 2024.

W. Wu, D. Wu, Y. Zhang, and W. Zhang are with the Department of Automation, Shanghai Jiao Tong University, Shanghai 200240, China (e-mail: wentao-wu@sjtu.edu.cn; sjtuwudi@sjtu.edu.cn; zhang297@sjtu.edu.cn; wdzhang@sjtu.edu.cn).

S. Chen is with the Department of Information and Communication Engineering, Hainan University, Haikou 570288, China (e-mail: skchen@hainanu.edu.cn).

Color versions of one or more of the figures in this paper are available online at http://ieeexplore.ieee.org.

Digital Object Identifier 10.1109/JAS.2023.123864

$$\bar{e}_{ir} = e_{ir} + \eta_{ir},\ \ \bar{e}_{il} = e_{il} + \eta_{il}. \tag{4}$$

In accordance with the PPC methodology, the tracking error $e_i \in (-\bar{e}_{il}, \bar{e}_{ir})$ is equivalently transformed into an unconstrained variable $\zeta_i \in (-\infty, \infty)$ through the following ETF:

$$T(\zeta_i) = (2e_i - \bar{e}_{ir} + \bar{e}_{il})(\bar{e}_{ir} + \bar{e}_{il})^{-1} \tag{5}$$

satisfying $\lim_{\zeta_i \mapsto \infty} T(\zeta_i) = 1$, $\lim_{\zeta_i \mapsto -\infty} T(\zeta_i) = -1$. By solving the inverse function of $T(\zeta_i(t)) = 2/\pi \arctan(\zeta_i)$, the variable ζ_i with the ETF (5) is given below:

$$\zeta_i = \tan\left(\pi(2e_i - \bar{e}_{ir} + \bar{e}_{il})(\bar{e}_{ir} + \bar{e}_{il})^{-1}/2\right). \tag{6}$$

Let $\Lambda_i = \partial\zeta_i/\partial e_i$, $\Lambda_{ir} = \partial\zeta_i/\partial e_{ir}$, and $\Lambda_{il} = \partial\zeta_i/\partial e_{il}$ from (6). According to (4) and (6), it gets that the time derivative of ζ_i is presented as $\dot{\zeta}_i = \Lambda_i\dot{e}_i + \Lambda_{ir}(\dot{e}_{ir} + \dot{\eta}_{ir}) + \Lambda_{il}(\dot{e}_{il} + \dot{\eta}_{il})$, $i = 1, 2$, where η_{ir} and η_{il} are updated with respect to the dynamics

$$\begin{aligned} \dot{\eta}_{ir} &= -\Lambda_{ir}^{-1}\Lambda_i(-\kappa_i\eta_{ir} + \tau_{ir}),\ \ \eta_{ir}(t_0) = 0 \\ \dot{\eta}_{il} &= \Lambda_{il}^{-1}\Lambda_i(-\kappa_i\eta_{il} + \tau_{il}),\ \ \eta_{il}(t_0) = 0 \end{aligned} \tag{7}$$

where κ_i is a positive constant; τ_{ir}, τ_{il} are inputs, to deal with inflexible bounds and collision avoidance, established as $\tau_{ir} = \tau_{il} = \frac{1}{2}(\mathrm{sign}(\rho) + 1)(\exp(\rho') - 1)$ where $\rho = \iota R_o - d_o$ and $\rho' = \rho/(d_o - R_o)$ with a positive constant ι and relative distance $d_o = \sqrt{(x_o - x)^2 + (y_o - y)^2}$. From [22], the properties of (7) are given by the following lemma, and proof is omitted due to limited space.

Lemma 1: Consider the MR (1), ETF (5) and FPF (4) with modified signals updated by (7). If the inequality $\|\tau_i\| \le \bar{\tau}_i$ and (3) hold for $\forall t \ge t_0$ with $\tau_i = \mathrm{col}(\tau_{ir}, \tau_{il})$ and $\bar{\tau}_i \in \mathbb{R}^+$, then $0 \le \eta_{ir}, \eta_{il} \le k_{rl}\bar{\tau}_i$ with k_{rl} being a positive constant.

Since $x_e = e_1\cos\varphi_d$ and $y_e = e_1\sin\varphi_d$ from (2), the desired guidance laws under guaranteed performance are designed as

$$\begin{aligned} u^* &= \Lambda_1^{-1}(L_1\zeta_1 + \Lambda_{1r}\dot{e}_{1r} + \Lambda_{1l}\dot{e}_{1l}) + \dot{x}_d\cos(\varphi_d) \\ &\quad + \dot{y}_d\sin(\varphi_d) + 2u\sin^2(0.5e_2) + \kappa_1(\eta_{1r} - \eta_{1l}) \\ w^* &= \Lambda_2^{-1}(L_2\zeta_2 + \Lambda_{2r}\dot{e}_{2r} + \Lambda_{2l}\dot{e}_{2l}) + \dot{\varphi}_d \\ &\quad + \kappa_2(\eta_{2r} - \eta_{2l}) \end{aligned} \tag{8}$$

where L_1 and L_2 are positive control gains.

Safety-critical angle speed guidance law: Based on the heading avoidance principle [23], a position-heading CBF is established as

$$h_o = \|p - p_o\|^2 - \beta_o\cos^2(\varphi - \varphi_o) - (R_o + \rho_o)^2 \tag{9}$$

where β_o is a positive constant; $\varphi_o = \mathrm{atan2}(y_o - y, x_o - x)$ is a relative angle of MR from obstacles.

To achieve the collision-free tracking, it ensures the forward invariance of a set $C_o = \{p \in \mathbb{R}^2 \mid h_o \ge 0\}$. Then, the safety of closed-loop system (1) can be guaranteed with the angle speed satisfying [13]

$$\mathcal{W}_{\mathrm{CBF}}(w) = \{w \in \mathbb{R} \mid \dot{h}_o + \alpha(h_o) \ge 0\} \tag{10}$$

where $\alpha(\cdot)$ is a class $\mathcal{K}$ function.

For the prescribed performance tracking problem of MRs in a dynamic environment, the safe constraints must be not violated under any condition. Based on the guidance law w^*, a safety-critical angle speed guidance law can be calculated by the following quadratic program:

$$\begin{aligned} w_{\mathrm{opt}} = &\ \arg\min_{w}\ 0.5\|w - w^*\|^2 \\ &\text{s.t.}\quad A_{\mathrm{CBF}}w \le b_{\mathrm{CBF}} \end{aligned} \tag{11}$$

where $A_{\mathrm{CBF}} = \beta_o\sin(2(\varphi - \varphi_o))$ and $b_{\mathrm{CBF}} = 2(p^T - p_o^T)(\dot{p} - \dot{p}_o) - 2\beta_o\sin(2(\varphi - \varphi_o))\dot{\varphi}_o$.

In this letter, we only focus on the safe guidance at the kinematic level. Thus, the following assumption is needed for kinetic controller.

Assumption 1: The kinetic controller of MRs perfectly track the desired signals such that $u = u^*$ and $w = w_{\mathrm{opt}}$.

By (1) and (2), one has $\dot{e}_1 = \dot{x}_d\cos(\varphi_d) + \dot{y}_d\sin(\varphi_d) - u + 2u\sin(0.5e_2)$ and $\dot{e}_2 = \dot{\varphi}_d - w$. Substituting $\dot{e}_1$, $\dot{e}_2$, u^* and w^* into $\dot{\zeta}_i$, it follows:

$$\dot{\zeta}_1 = -L_1\zeta_1,\ \ \dot{\zeta}_2 = -L_2\zeta_2 + \Lambda_2 w_e \tag{12}$$

with $w_e = w^* - w_{\mathrm{opt}}$. The stability of system (12) is stated by Lemma 2.

Lemma 2: Under Assumption 1, the system (12): $[w_e] \to [\zeta_1, \zeta_2]$ is input-to-state stable.

Proof: Consider a Lyapunov function candidate as $V = (\zeta_1^2 + \zeta_2^2)/2$ and take its derivative $\dot{V} = -L_1\zeta_1^2 - L_2\zeta_2^2 + \zeta_2\Lambda_2 w_e$. Letting $\zeta = \mathrm{col}(\zeta_1, \zeta_2)$, $L = \mathrm{diag}\{L_1, L_2\}$, one has $\dot{V} \le -(1-\epsilon)\lambda_{\min}(L)\|\zeta\|^2 - \epsilon\lambda_{\min}(L)\|\zeta\|^2 + \|\zeta\||\Lambda_2 w_e|$. Since $\|\zeta\| \ge |\Lambda_2 w_e|/(\epsilon\lambda_{\min}(L))$, one has $\dot{V} \le -(1-\epsilon)\lambda_{\min}(L)\|\zeta\|^2$. According to [24, Theorem 4.6], system (12) is input-to-state stable, and the ultimate bound is expressed as $\|\zeta(t)\| \le \max\{\|\zeta(t_0)\|\exp(-(1-\epsilon)(t-t_0)), |\Lambda_2 w_e|/(\epsilon\lambda_{\min}(L))\}$, $\forall t \ge t_0$. The stability and safety of proposed system (12) are stated by the following theorem. ■

Theorem 1: Consider a MR system (1) with the desired guidance laws (8) and the safety-critical angle speed (11). Under Assumption 1, all errors evolve within flexible performance functions (4), and the closed-loop system is safe if $p(t_0) \in C_o$.

Proof : From Lemma 2, it is concluded that error e_i is bounded and satisfies FPF constraints (4), i.e., the first objective is achieved. According to [13], $p(t_0) \in C_o$ and $w \in \mathcal{W}_{\mathrm{CBF}}(w)$ render the forward invariance of C_o. Then, the safety of MR is ensured, i.e. the second objective is achieved. ■

Simulation and experiment results: In this section, a simulation example with comparison analysis and an experiment example are provided to verify the effectiveness and feasibility of the proposed method.

Simulation results: Consider a MR to track a predefined time-varying trajectory $p_d(t) = \mathrm{col}(0.5t, -10\sin(0.05t))$ from initial status $(-10, -8, 0.5\pi)$. Two stationary obstacles with $o = 1, o = 2$ and one dynamic obstacle with $o = 3$ are arranged at $p_1 = (40, 5)$, $p_2 = (70, -10)$ and $p_3 = (170 - 0.2t, 0)$, respectively. Other parameters are set as $\delta_{ir} = \delta_{il} = 0.6$, $\varrho_{10} = 13$, $\varrho_{20} = 1$, $\varrho_{1\infty} = 0.5$, $\varrho_{2\infty} = 0.1$, $\mu_1 = 0.2$, $\kappa_1 = 0.5$, $\kappa_2 = 1$, $L_1 = 0.2$, $L_2 = 2.0$, $\beta_o = 1$, and $\alpha(h_o) = 0.5h_o$.

Figs. 1–5 display the simulation results concluding the comparison results with the method in [9]. From snapshots at different moments in Fig. 1, it follows that the MR can track the desired trajectory $p_d(t)$ while successfully avoiding all obstacles. In Figs. 2(a) and 2(c), it is seen that errors e_1 and e_2 using our proposed method show obvious hills or volatility when collision avoidance occurs, but still evolve within the corresponding prescribed space $(-\bar{e}_{il}, \bar{e}_{ir})$, $i = 1, 2$. To deal with these tracking degradations, the auxiliary system (7) generates the positive modification variables η_{1r}, η_{1l}, η_{2r}, and η_{2l} in Fig. 3. Compared with the method in [9], the error e_2 arrives at the inflexible boundary $-e_{2l}$ in Fig. 2(d). As shown in Fig. 4(b), the distance curve $\|p - p_o\|$ between MR and each obstacle crosses the safe lines defined by $R_o + \rho_o$, $o = 1, 2, 3$ when encountering the stationary/dynamic obstacle. It means that the signal w^* cannot ensure the safety of the MR. From Fig. 4(a), the safety-critical angle speed w_{opt} can

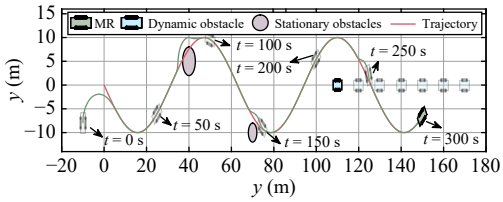

Fig. 1. Snapshots in 0 s, 50 s, 150 s, 200 s, 250 s, and 300 s.

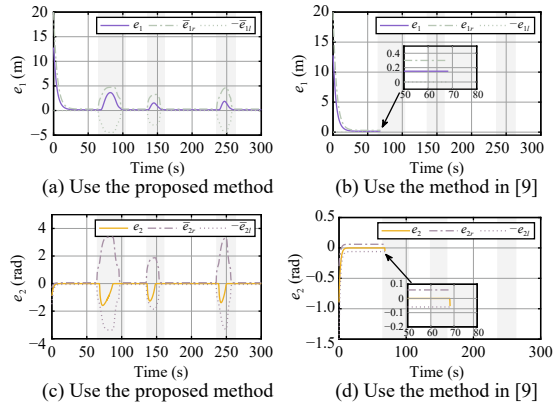

(a) Use the proposed method (b) Use the method in [9]

(c) Use the proposed method (d) Use the method in [9]

Fig. 2. The relative distance and heading error with guaranteed performance.

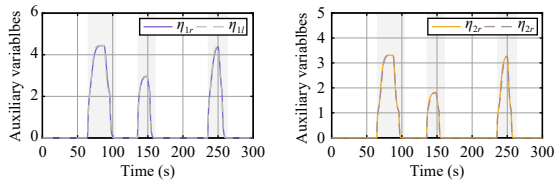

Fig. 3. The state responses of auxiliary systems.

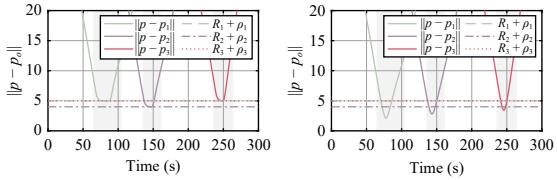

(a) With w_{opt} (b) With w^*

Fig. 4. The distances between MR and each obstacle with and without CBFs.

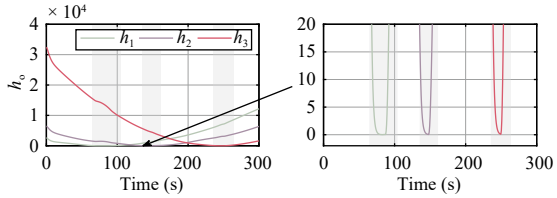

Fig. 5. The position-heading CBFs (9) of MR subject o each obstacle.

guarantee that all curves $\|p-p_o\|$, $o=1,2,3$ lie above the safe lines. In Fig. 5, the position-heading CBFs (9) for all obstacles are always above $h_o=0$. It is further concluded that there is no collision during the tracking process.

Experiment results: In order to further verify the feasibility of the proposed method, an experimental example is given with a mecanum-wheel-driven MR based on an experimental platform in Fig. 6. A static obstacle is set at (0.5, 1.2), and its motion position can be obtained from an optical capture system in Fig. 6. Conducted by the above simulation example, experiment results are plotted in Figs. 7 and 8. Fig. 7 draws the actual tracking trajectory of MR and a trajectory snapshot from the optical capture system based on our proposed method. From Fig. 8, it follows that MR successfully avoids the potential collision since the curve $\|p-p_o\|$ with w_{opt} is always above the line $R_1+\rho_1$. It is further proved by the positive CBF h_o in Fig. 8.

Conclusion: This letter proposed a safety-critical performance-guaranteed trajectory tracking method for MRs operating in an obstacle environment. The relative distance and heading errors can converge the neighbors of the origin with respect to the user-specified performance constraints. Using the designed position-heading CBF, collision-free trajectory tracking is achieved for MRs. Additionally, the tracking errors do not violate FPF constraints by utilizing the proposed auxiliary system. Simulation and experiment results show the effectiveness and superiority of the proposed control method.

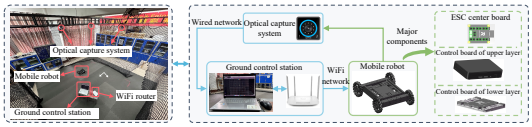

(a) Experiment rig (b) Hardware structure

Fig. 6. The experiment platform for the developed control scheme.

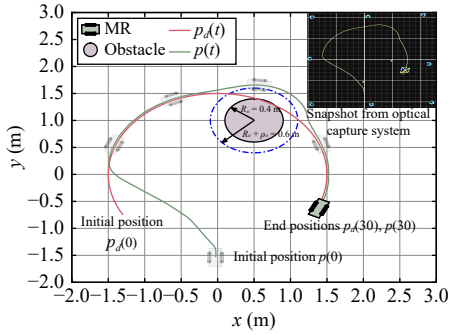

Fig. 7. The safety-critical tracking of MR in the experiment.

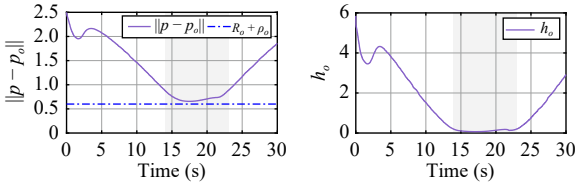

Fig. 8. The relative distance and the position-heading CBF in the experiment.

Acknowledgments: This work was supported in part by the National Key R&D Program of China (2022ZD0119901), the Shanghai Science and Technology Program (22015810300), the Hainan Province Science and Technology Special Fund (ZDYF2024GXJS 003), and the National Natural Science Foundation of China (U2141234, 52201369).

References

[1] J. Wang, J. Wang, and Q.-L. Han, "Receding-horizon trajectory planning for under-actuated autonomous vehicles based on collaborative neurodynamic optimization," *IEEE/CAA J. Autom. Sinica*, vol. 9, no. 11, pp. 1909–1923, 2022.

[2] Z. Peng, J. Wang, D. Wang, and Q.-L. Han, "An overview of recent advances in coordinated control of multiple autonomous surface vehicles," *IEEE Trans. Ind. Informat.*, vol. 17, no. 2, pp. 732–745, 2021.

[3] T. Liu and Z.-P. Jiang, "Distributed formation control of nonholonomic mobile robots without global position measurements," *Automatica*, vol. 49, no. 2, pp. 592–600, 2013.

[4] Z. Li, C. Yang, C.-Y. Su, J. Deng, and W. Zhang, "Vision-based model predictive control for steering of a nonholonomic mobile robot," *IEEE Trans. Control Syst. Technol.*, vol. 24, no. 2, pp. 553–564, 2015.

[5] X. Ge, Q.-L. Han, J. Wang, and X.-M. Zhang, "A scalable adaptive approach to multi-vehicle formation control with obstacle avoidance," *IEEE/CAA J. Autom. Sinica*, vol. 9, no. 6, pp. 990–1004, 2021.

[6] C. P. Bechlioulis and G. A. Rovithakis, "Robust adaptive control of feedback linearizable MIMO nonlinear systems with prescribed performance," *IEEE Trans. Autom. Control*, vol. 53, no. 9, pp. 2090–2099, 2008.

[7] M. Chen, "Disturbance attenuation tracking control for wheeled mobile robots with skidding and slipping," *IEEE Trans. Ind. Electron.*, vol. 64, no. 4, pp. 3359–3368, 2016.

[8] D. Fu, J. Huang, and H. Yin, "Controlling an uncertain mobile robot with prescribed performance," *Nonlinear Dyn.*, vol. 106, no. 3, pp. 2347–2362, 2021.

[9] W. Wu, Y. Zhang, W. Zhang, and W. Xie, "Distributed finite-time performance-prescribed time-varying formation control of autonomous surface vehicles with saturated inputs," *Ocean Eng.*, vol. 266, p. 112866, 2022.

[10] K. Lu, S.-L. Dai, and X. Jin, "Fixed-time rigidity-based formation maneuvering for nonholonomic multirobot systems with prescribed performance," *IEEE Trans. Cybern.*, vol. 54, no. 4, pp. 2129–2141, 2024.

[11] S. He, M. Wang, S. Dai, and F. Luo, "Leader-follower formation control of USVs with prescribed performance and collision avoidance," *IEEE Trans. Ind. Informat.*, vol. 15, no. 1, pp. 572–581, 2019.

[12] S.-L. Dai, K. Lu, and X. Jin, "Fixed-time formation control of unicycle-type mobile robots with visibility and performance constraints," *IEEE Trans. Ind. Electron.*, vol. 68, no. 12, pp. 12615–12625, 2020.

[13] A. D. Ames, X. Xu, J. W. Grizzle, and P. Tabuada, "Control barrier function based quadratic programs for safety critical systems," *IEEE Trans. Autom. Control*, vol. 62, no. 8, pp. 3861–3876, 2016.

[14] L. Wang, A. D. Ames, and M. Egerstedt, "Safety barrier certificates for collisions-free multirobot systems," *IEEE Trans. Robot.*, vol. 33, no. 3, pp. 661–674, 2017.

[15] S. Gao, Z. Peng, H. Wang, L. Liu, and D. Wang, "Safety-critical model-free control for multi-target tracking of USVs with collision avoidance," *IEEE/CAA J. Autom. Sinica*, vol. 9, no. 7, pp. 1323–1326, 2022.

[16] N. Gu, D. Wang, Z. Peng, and J. Wang, "Safety-critical containment maneuvering of underactuated autonomous surface vehicles based on neurodynamic optimization with control barrier functions," *IEEE Trans. Neural Netw. Learn. Syst.*, vol. 34, no. 6, pp. 2882–2895, 2023.

[17] W. Wu, Y. Zhang, W. Zhang, and W. Xie, "Output-feedback finite-time safety-critical coordinated control of path-guided marine surface vessels based on neurodynamic optimization," *IEEE Trans. Syst. Man, Cybern., Syst.*, vol. 53, no. 3, pp. 1788–1800, 2023.

[18] W. Wu, Z. Peng, L. Liu, and D. Wang, "A general safety-certified cooperative control architecture for interconnected intelligent surface vehicles with applications to vessel train," *IEEE Trans. Intell. Veh.*, vol. 7, no. 3, pp. 627–637, 2022.

[19] N. Gu, Z. Peng, D. Wang, and F. Zhang, "Path-guided containment maneuvering of mobile robots: Theory and experiments," *IEEE Trans. Ind. Electron.*, vol. 68, no. 8, pp. 7178–7187, 2020.

[20] S.-L. Dai, S. He, M. Wang, and C. Yuan, "Adaptive neural control of underactuated surface vessels with prescribed performance guarantees," *IEEE Trans. Neural Netw. Learn. Syst.*, vol. 30, no. 12, pp. 3686–3698, 2018.

[21] W. Wu, Z. Peng, D. Wang, L. Liu, and Q.-L. Han, "Network-based line-of-sight path tracking of underactuated unmanned surface vehicles with experiment results," *IEEE Trans. Cybern.*, vol. 52, no. 10, pp. 10937–10947, 2022.

[22] R. Ji, D. Li, J. Ma, and S. S. Ge, "Saturation-tolerant prescribed control of mimo systems with unknown control directions," *IEEE Trans. Fuzzy Syst.*, vol. 30, no. 12, pp. 5116–5127, 2022.

[23] L. Liu, Y. Xu, Z. Huang, H. Wang, and A. Wang, "Safe cooperative path following with relative-angle-based collision avoidance for multiple underactuated autonomous surface vehicles," *Ocean Eng.*, vol. 258, p. 111670, 2022.

[24] H. K. Khalil, *Nonlinear Control*. London, UK: Pearson, 2015.